Proximity Operations Sensors Demonstration, SpaceTech-REDDI-2021

Program Final Report

December 16th, 2024

Prepared by:

Stefan Bieniawski, Nathan Powel, and Mark Villela
Blue Origin, LLC
Kent, WA

The material is based upon work supported by the National Aeronautics and Space Administration under Contract Number 80NSSC22K0842.

Any opinions, findings, and conclusions or recommendations expressed in this material are those of the author(s) and do not necessarily reflect the views of the National Aeronautics and Space Administration.

ABSTRACT

This document provides the final report on the Proximity Operations Sensors Demonstration SpaceTech-REDDI-2021 program, a public-private partnership between Blue Origin and NASA that is partially funded by NASA contract 80NSSC22K0842. In this report, we summarize the results of the entire contract, including recommendations and conclusions based on the experience and results obtained.

The scope of this document is a discussion of all the major tasks performed under the contract, including the sensor flight demonstrations on New Shepard. Two sensor demonstration flights were completed, one for the vision-based navigation sensing demonstration and one for ultrawideband sensing proximity operations and landing sensing demonstrations.

TABLE OF CONTENTS

LIST OF FIGURES

ACRONYMS

BET	Best-estimate trajectory
CC	Crew Capsule
CLAHE	Contrast-limited adaptive histogram equalization
COTS	Commercial off the shelf
dB	Decibel
GHz	Gigahertz
GNSS	Global Navigation Satellite System
GPS	Global Positioning System
HWIL	Hardware-In-the-Loop
km	Kilometer(s)
LSO	Launch Site One
m	Meter(s)
m^2	Square meters
m/s	Meters per second
mm	millimeter
MET	Mission elapsed time
NASA	National Aeronautics and Space Administration
NS	New Shepard
PM	Propulsion Module
RF	Radio frequency
RPO	Rendezvous and proximity operations
s	Second(s)
SNR	Signal-to-Noise Ratio
TRL	Technology readiness level
UWB	Ultrawideband
VBN	Vision-based navigation
W	Watt

REFERENCES

[1] Utilizing Public-Private Partnerships to Advance Tipping Point Technologies, Appendix Number: 80HDTR18NOA01-18STDM_001, Amendment 5, November 30, 2017.

[2] Olson, Edwin. "AprilTag: a robust and flexible visual fiducial system," IEEE International Conference on Robotics and Automation, Shanghai, China, May 2011. Pg. 3400-3407. doi: 10.1109/ICRA.2011.5979561.

1. INTRODUCTION

1.1. Background

Rendezvous and proximity operations (RPO) will be a consistent feature of future crewed and un-crewed missions in low Earth orbit, cislunar space, at the Moon, and beyond. Existing sensor approaches for RPO operations are centered on lidar, which is demanding in terms of size, weight, power, and cost. Alternate sensors for RPO with lower cost and low size, weight, and power have the potential to support a variety of missions and to expand the ecosystem of cislunar activity.

As a SpaceTech-REDDI-2021 awardee, Blue Origin proposed to investigate two low-cost, low TRL lidar alternatives for RPO and powered landing sensing: an ultrawideband (UWB) ranging sensor and a vision-based navigation (VBN) camera. Both sensors have lower size, weight, and power than existing sensors, and substantially lower cost as well. These novel sensors can potentially improve RPO capabilities and operations in LEO, cislunar space, and at the Gateway in particular. The ultrawideband ranging sensor also increases robustness by avoiding lighting challenges and, in the role of a backup, provides dissimilar sensing to avoid common mode faults. The UWB also provide a backup communication link for proximity data.

UWB ranging sensors make round-trip time-of-flight measurements between multiple sensor locations at up to several hundred meters range, accurate to a few centimeters, with up to 125Hz rate. In an RPO application, several sensors are placed in a pattern on the target vehicle, allowing a chase vehicle equipped with one sensor to determine its position relative to the target to within a few centimeters when at close range, and to determine accurate range to the target at longer ranges. Each sensor is approximately 160x75x50 mm and draws less than 3 W of power. These sensors have terrestrial industrial applications but have not been used in space. The larger (e.g., robotics) market for these sensors results in lower cost than dedicated RPO sensors.

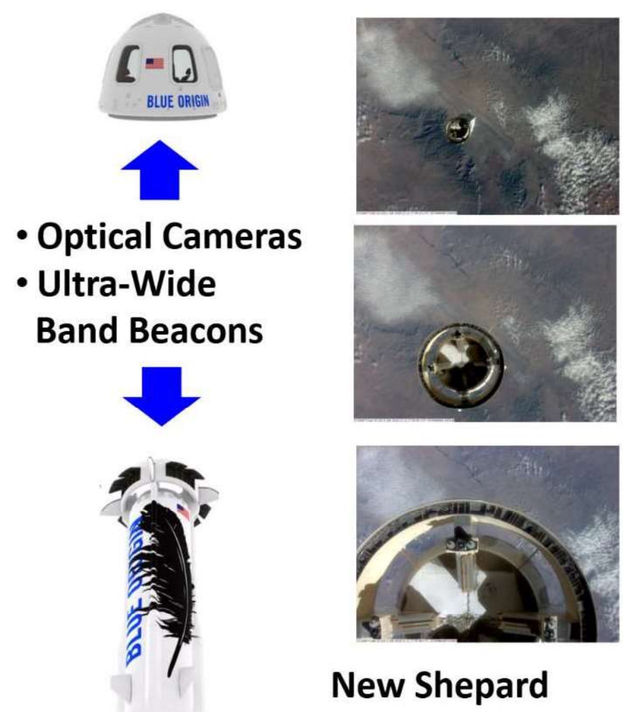

Figure 1: Proximity operations sensing demonstration overview.

Vision-based navigation involves using a camera to detect passive fiducial markers (i.e., points of reference) on a target vehicle. By taking bearings to multiple fiducials, or multiple points within a large fiducial, the relative position and attitude of the chase vehicle can be determined. The camera is compact and low power. Moreover, many vehicles already require cameras (e.g., to provide crew docking assistance), meaning that additional sensors may not be required for vision-based navigation. The substantial market for cameras, and even space-rated cameras, results in substantially reduced costs.

While neither technology under investigation has the sensing range of lidars in existing use (several kilometers), they have substantial advantages in other metrics such as size, weight, power, and cost. This effort provides data to confirm the performance of the proposed sensors in measurement range and accuracy relative to their size, weight, and power.

The Proximity Operations Sensors Demonstration (SpaceTech-REDDI-2021) included integration of ultrawideband ranging transceivers and passive fiducials on the New Shepard Propulsion Module and ultrawideband transceivers on the Crew Capsule and at the New Shepard Landing Pad to demonstrate low-cost, low-TRL sensors in proximity and landing operations. An existing camera on the Crew Capsule was calibrated and provided observations for the VBN experiment. Figure 1 shows the Propulsion Module and Crew Capsule and the separation environment for the proximity sensors demonstration.

The principal objective of this flight test program is to advance the TRL for these sensors from TRL 4 to TRL 6 by demonstrating them in mission relevant environments aboard New Shepard. Specifically, our flight test objectives were:

- Sensors operate on the vehicle and in space relevant environments.
- Sensors record data throughout vehicle separation, and, for the UWB sensors only, throughout landing.
- Collect flight data that can be used to estimate the relative position of the PM and CC.
- Operational range and accuracy of each sensor type to be determined.

Each of these mission objectives were accomplished.

1.2. Document Overview

This final report combines the summaries of the work completed under the three experiments described in the SpaceTech-REDDI-2021 proposal. In Section 2 we provide an overview of the UWB RPO sensor experiment, including a summary of the mission profile, and describe the results of the experiment. Section 3 contains an overview and the results of the UWB landing sensor experiment, which was conducted on the same flight. Section 4 describes the VBN RPO sensor experiment. We conclude in Section 5 with the program level conclusions and recommendations.

2. ULTRAWIDEBAND RPO SENSING OBJECTIVE

2.1. Overview

The ultrawideband RPO sensing experiment was designed to test ultrawideband ranging transceivers during separation of the New Shepard Propulsion Module and Crew Capsule in relevant space environments. The geometry of the UWB installation was chosen to provide direct line-of-sight from the PM to the CC sensors during separation and to enable trilateration of the CC position relative to the PM after separation.

Three UWB sensors were installed on the top of the Propulsion Module, as shown in Figure 2, near the outside edge of the PM "tabletop", inside the ring-fin. UWBs were installed on aluminum plates that matched UWB and PM fastener patterns and served as a back-reflectors for the UWB antennas. This installation location directly exposed the UWB sensors to space environments during the mission. Power for the PM UWBs was provided from payload batteries under the tabletop.

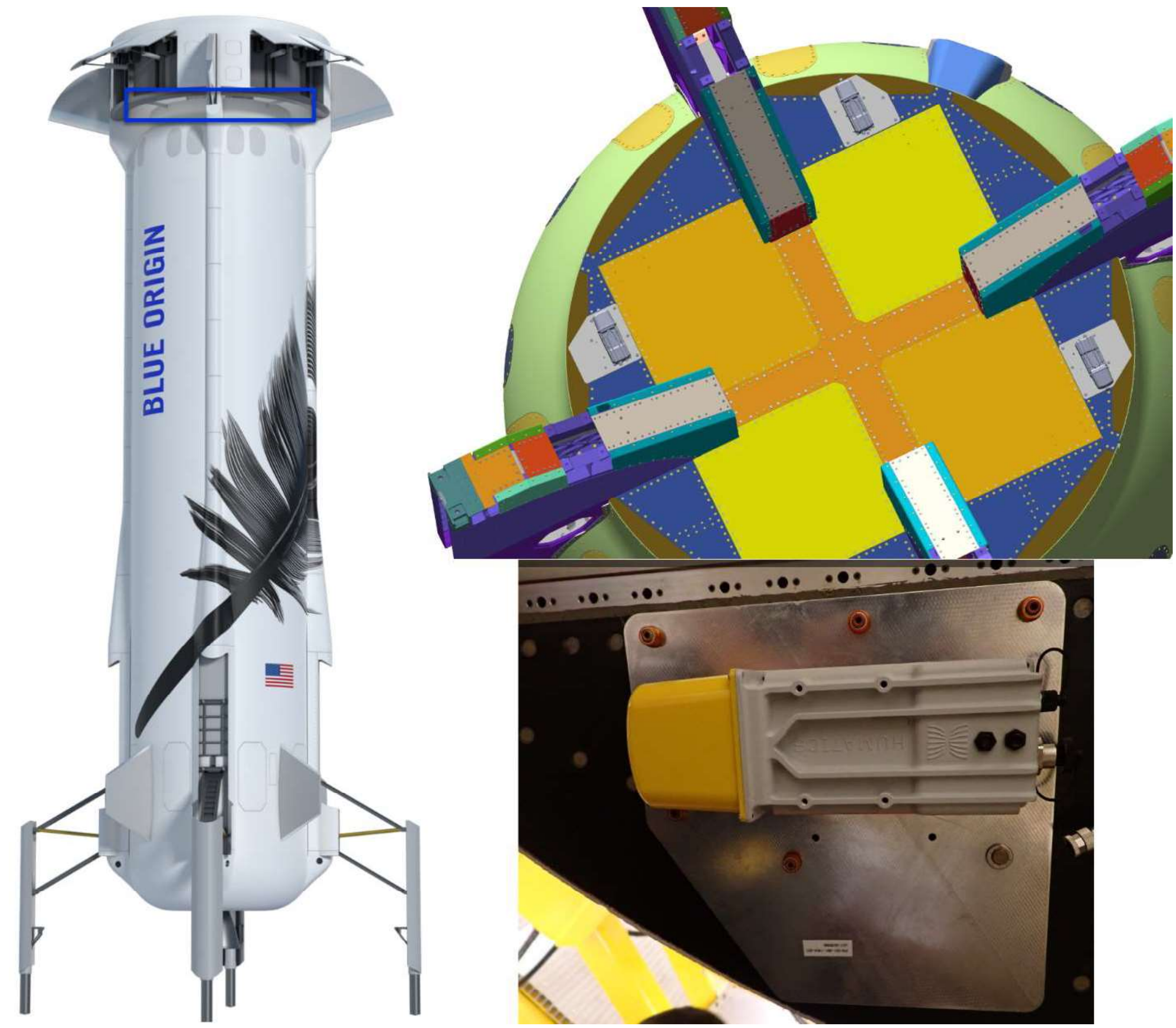

Figure 2: Three UWB sensors installed on the top of the New Shepard Propulsion Module (blue boxed area), distributed to provide as wide as possible of a ranging baseline.

One UWB sensor was installed in the aft compartment of the New Shepard Crew Capsule as shown in Figure 3. The UWB antenna was installed directly behind an aft-facing window in the Crew Capsule base heat shield to maximize RF signal-strength at the Propulsion Module. However, space constraints required the UWB chassis to be installed several feet away, with a coaxial cable connection to the antenna. After calibration, a signal delay of 10.2 ns was configured in the UWB software to compensate for the additional harness length. No back-reflector was provided for this antenna. Power for the CC UWB was provided from a dedicated battery in the CC cabin. Both PM and CC UWBs were installed horizontally, to maximize mutual RF signal-gain, but no attempt was made to control relative antenna polarization.

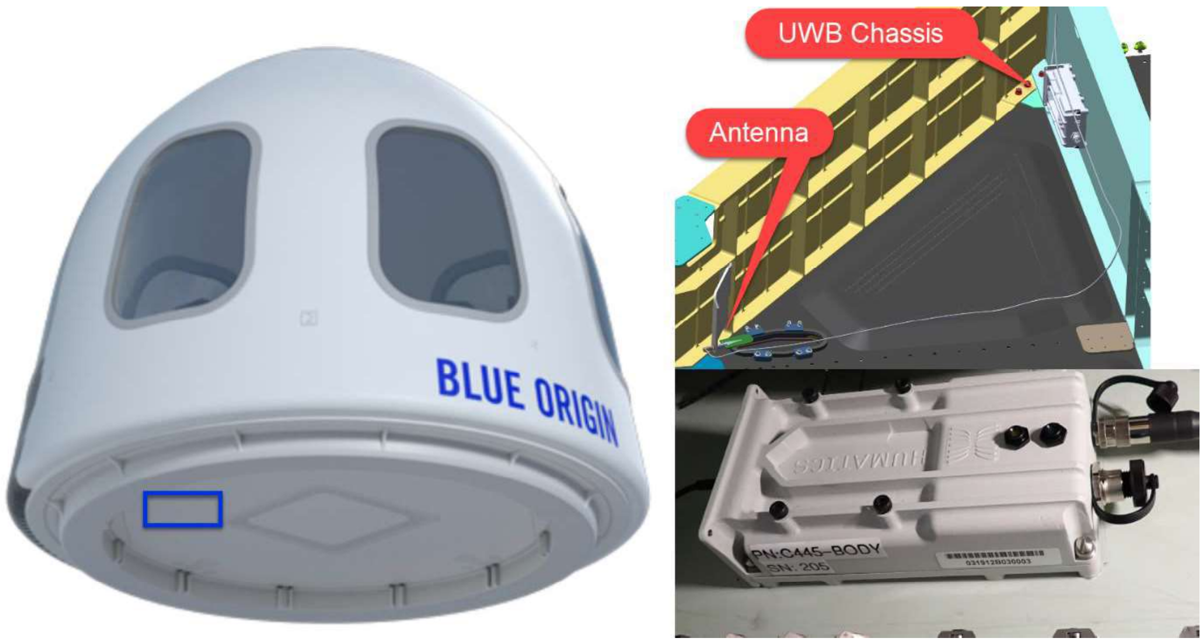

Figure 3: One UWB sensor installed in the aft portion of the New Shepard Crew Capsule. The UWB antenna was installed behind an aft-facing window near the edge of Crew Capsule base heat shield with the UWB sensor chassis installed on a nearby structural member.

During the mission, each of the PM UWBs took turns transmitting range requests to the CC UWB. The CC UWB did not emit signals, except in response to received range requests. Embedded in each range request was the last measured range. One UWB on the PM (the "primary UWB) relayed these range measurements to the PM payload data logging system. Only the primary UWB on the PM had an Ethernet connection to the PM payload data logger.

2.2. **Summary of Sensor Flight Demonstration**

2.2.1. NS-27: 23-October-2024

The morning of the NS-27 mission, the CC UWB was powered on prior to roll-out. Once at the launch stand, the landing pad UWBs and the PM UWBs were briefly powered on for systems checks and built-in-tests, then powered down again while propellant was loaded. One hour prior to launch, all UWB payloads were activated.

The New Shepard flight profile was nominal; the mission altitude profile is shown in Figure 4. Separation of the Propulsion Module and Crew Capsule took place around 70 km, in vacuum pressure, thermal, and illumination conditions. The PM and CC separated at approximately 1.5 m/s, providing simulated undocking RPO conditions for the UWB RPO sensing experiment.

After re-entry, the PM descended to just over the landing pad and began a constant velocity descent, shutting down the engine after touching down. After touchdown, the PM UWB payloads remained powered for approximately 5 minutes before being powered down. After the PM UWB powered off, the landing pad UWB (discussed in more detail in Section 3) were commanded to stop transmitting.

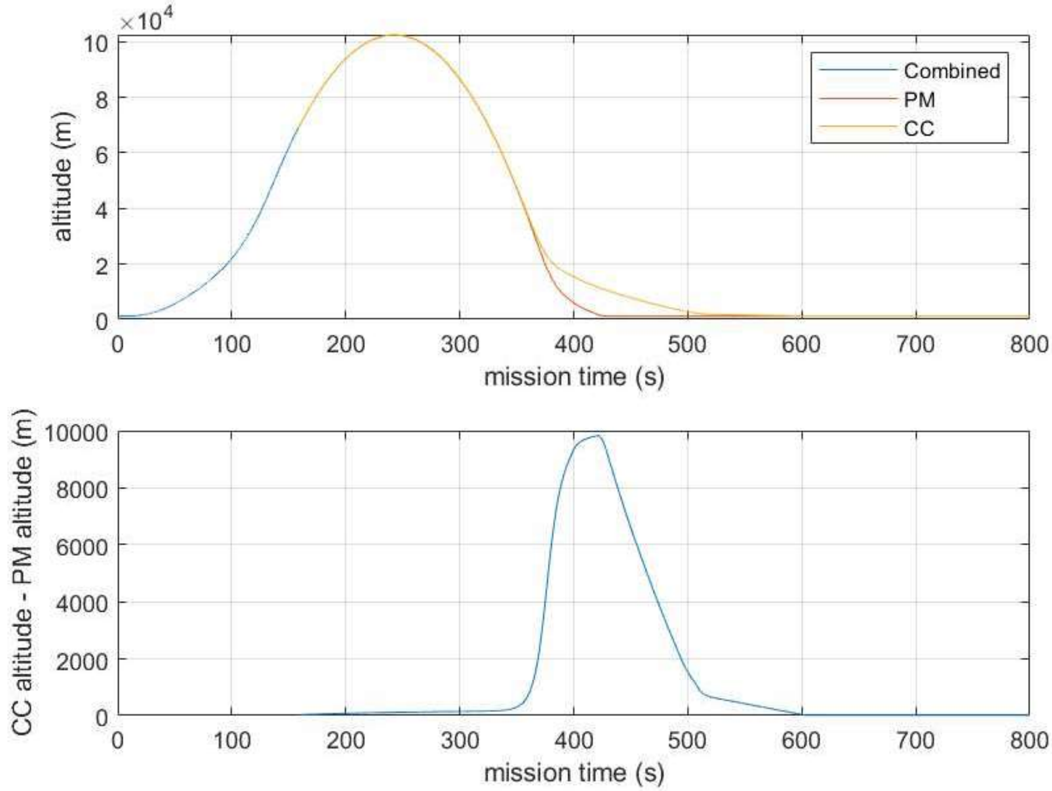

Figure 4: NS-27 New Shepard altitude profile and altitude separation between PM and CC

Data collected from the onboard navigation systems for each vehicle was processed into a best-estimate trajectory (BET), which represents the most accurate record of the vehicle's trajectory. The BET was used as a reference source for the UWB measurement performance. Post-flight inspection showed no damage, or any observable changes, to any of the UWB involved in the experiment.

2.3. **Key Results and Findings**

Prior to separation no reliable range measurements were obtained between the PM tabletop UWBs and the CC UWB. While the UWBs did report measurements, these measurements bounced between discrete bands spread from 0.28 to 6.4 m, characteristic of expected multipath interference, as shown in Figure 5. After separation, the noise in the measurements reduced substantially and generally tracked the BET well (see Figure 6), though separation velocity measured by the UWB was lower than measured in the BET. We have reason to believe that the BET relative trajectory includes a significant random-walk component that could impact the measurement of the separation velocity. UWB range measurements cut off after about 10 m, lower than expected.

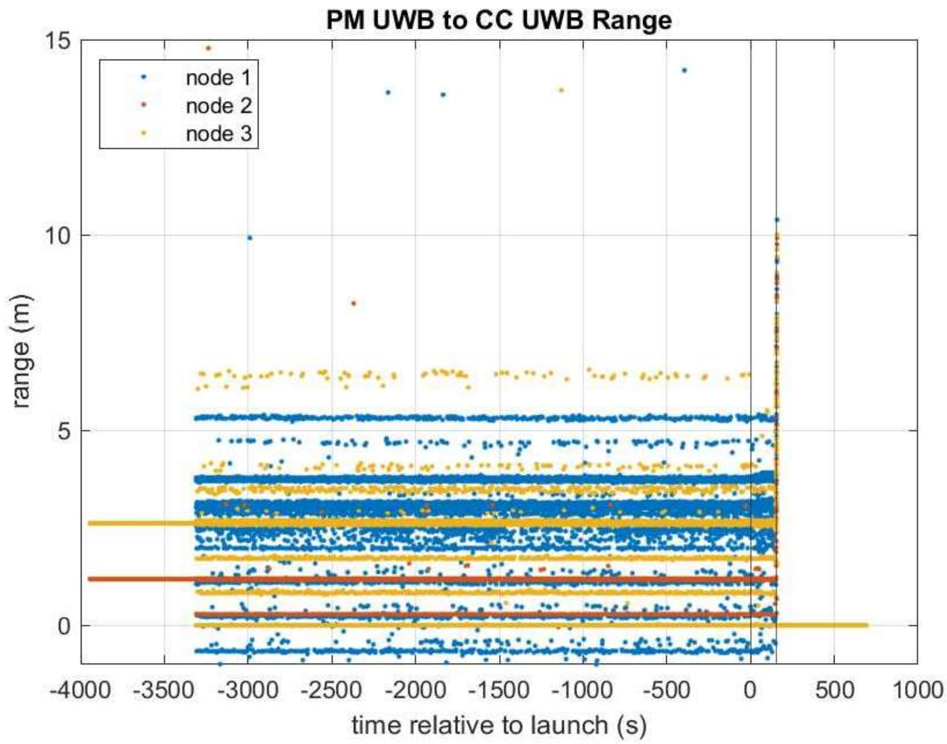

Figure 5: Range measurements between PM UWBs and CC UWB with markers at launch and separation.

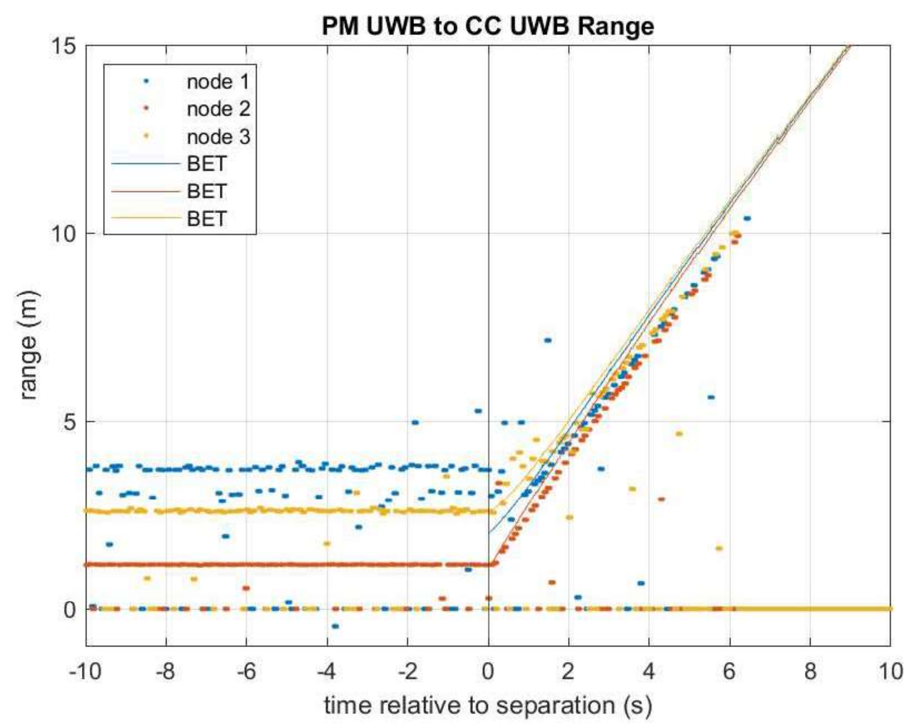

Figure 6: Range measurements between the PM UWBs and CC UWB at separation.

Sensor SNR was steady prior to separation but began dropping as the PM and CC separated (see Figure 7). Below about 18 dB, no range measurements were obtained.

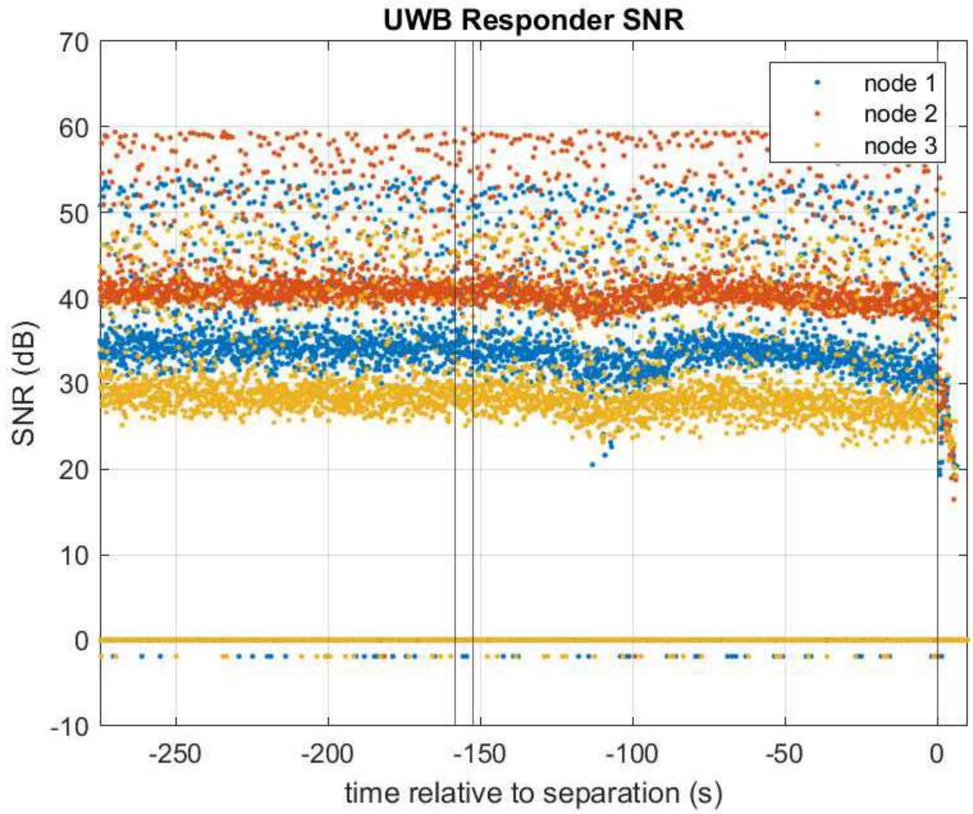

Figure 7: SNR between the PM UWBs and CC UWB with vertical lines at engine ignition, launch, and separation.

2.4. Conclusions and Recommendations

The most significant finding in this experiment is that the maximum range realized by the UWB was substantially lower than expected. The device specification lists a range of up to 500 m. Given integration limitations, we had expected to get range measurements out to around 100 m. Instead, a substantial drop in SNR occurred at under 10 m, preceding complete measurement loss. The most likely explanation for this underperformance is two-fold: 1) the experiment took place in an environment that promoted extreme amounts of multipath interference, and 2) that the RF signal between the PM UWBs and the CC UWB was attenuated by the CC base heat shield.

The location of the PM UWBs on the tabletop, while ideal for providing a direct line-of-sight to the bottom of the CC, also surrounds them by RF reflective surfaces on the ring-fin and the ring-fin supports, essentially putting them at the bottom of a tin can. Prior to separation, the aft end of the CC provides an additional RF reflective surface and closes the cavity. As a result, there are many paths for RF signals to take from the PM UWB to each other and to the CC UWB with only slightly different lengths, producing multipath interference. A dedicated RPO sensor integration would place the UWB sensors (or their antennas) above as much of the surrounding structure as possible to reduce this interference.

While the window in front of the CC UWB antenna was made of a material that was highly RF transparent, integration constraints limited the antenna to placement at the edge of the window, nearly 1" back from the inner face of the window. As a result, the field of view through the window was limited, and the most direct signal path from the CC UWB to the PM UWBs passed through the CC base heat shield, which most likely attenuated the signal. A dedicated RPO sensor integration with the CC UWB antenna on the outside of the structure or behind a dedicated radome would likely have substantially improved performance.

During the window immediately after separation when the UWB was providing range measurements, the measurements were accurate and low in noise. The range measurements from all three UWB were consistent. A tuned Chi-square rejection scheme could be used to eliminate clear outlier measurements.

Multipath interference is clearly a significant factor in the performance of UWB sensors for RPO sensing. While the integration environment on New Shepard was particularly pathological with respect to multipath, with the ring-fin and ring-fin supports in close proximity above the PM UWBs, great care will have to be taken in integrating UWB sensors on spacecraft to mitigate multipath interference. Given the low signal power used by UWB sensors, antennas should be integrated behind as little vehicle structure as possible, to mitigate signal attenuation. Those concerns aside, we demonstrate that UWB can provide accurate sensing of relative positioning for RPO applications.

3. ULTRAWIDEBAND LANDING SENSING OBJECTIVE

3.1. Overview

The ultrawideband landing sensing experiment was designed to test UWB transceivers during powered landing of the New Shepard Propulsion Module, including the impact of rocket exhaust and landing ejecta on system performance.

One UWB was installed in a PM ring-fin support fairing, as shown in Figure 8, on an aluminum bracket that held it at an angle to the ground that improved the RF gain near the edge of the landing pad and served as back-reflector. The PM ring-fin UWB installation was un-pressurized but protected from re-entry heating. Power was supplied by payload batteries beneath the tabletop.

Figure 8: One UWB sensor was installed in a New Shepard Propulsion Module ring-fin support (marked by the blue box), providing a view of the ground.

Three UWB sensors were installed on tripods around the northeast quadrant of the PM landing pad at Launch Site One, at the locations marked in Figure 9. The northeast quadrant was selected to maximize the probability of all three available UWBs having a direct line-of-sight to the side of the PM where the ring-fin UWB was installed, based on historical and modeled PM landing orientations, and to take advantage of existing ground power and networking infrastructure. Each UWB was installed approximately 53″ above the ground and approximately 250′ from the center of the landing pad. Power and data connections were provided by power-over-Ethernet connections to nearby ground infrastructure. Antenna orientation of the ground units was chosen to avoid aiming the null-axis of each UWB towards either the PM landing pad or other ground UWBs. After installation, the position of the phase center of the antenna of each UWB was measured by a survey-grade GPS receiver.

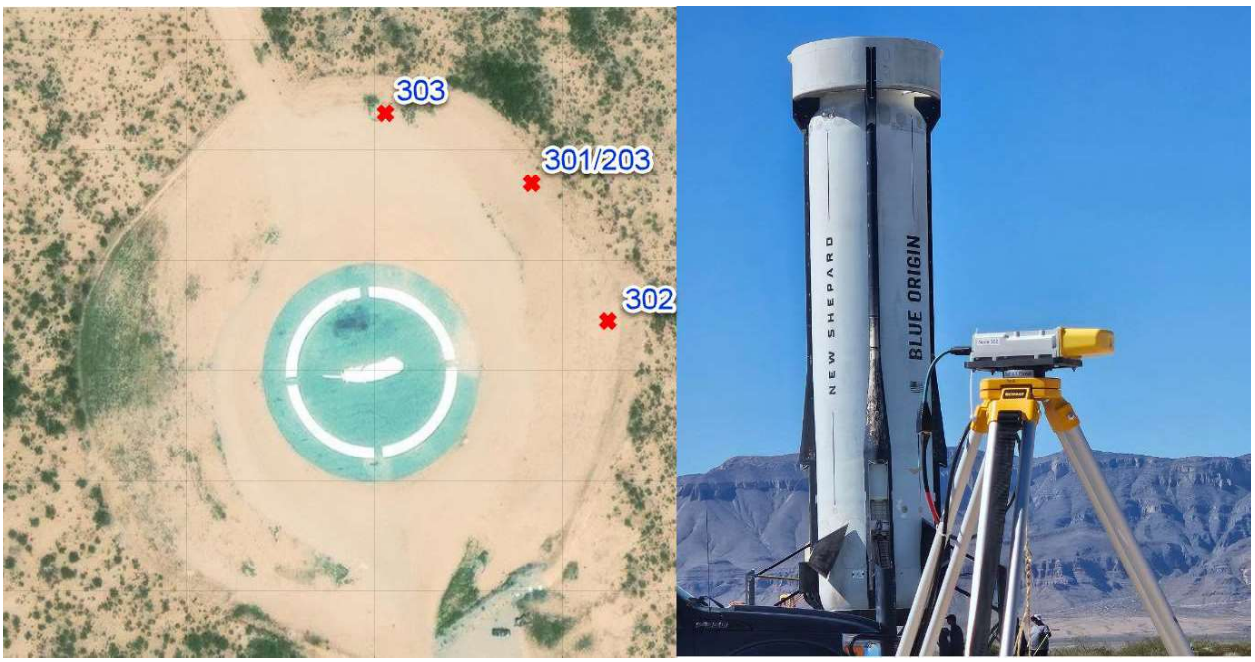

Figure 9: Three UWB sensors were installed on tripods around the NE quadrant of the landing pad at the locations marked with red X's, in view of the most probable landing orientation of the PM ring-fin UWB.

During the mission, each of the ground UWBs took turns transmitting range requests to the PM ring-fin UWB. Once the PM was sufficiently close the landing pad, the PM ring-fin UWB began responding to the range requests. Data was logged from all three ground UWBs on a ground console at Launch Site One.

The landing sensing demonstration took place in a different part of the mission timeline from the proximity operations demonstration. However, to mitigate the risk of interference between the two sets of UWBs, a separate RF channel was used for the landing sensing demonstration.

3.2. **Key Results and Findings**

First contact was made between the UWBs at the landing pad and the ring-fin UWB on the PM at a range of 265 m (corresponding to a PM altitude of 219 m). Initially, UWBs 301 and 302 received range responses (see Figure 10), but the northernmost UWB (303) did not begin receiving range responses from the PM ring-fin UWB until shortly before touchdown. The PM was rotating slowly counterclockwise during descent and landed with the ring-fin UWB facing west; by touchdown, UWBs 302 and 301 were no longer receiving responses from the PM.

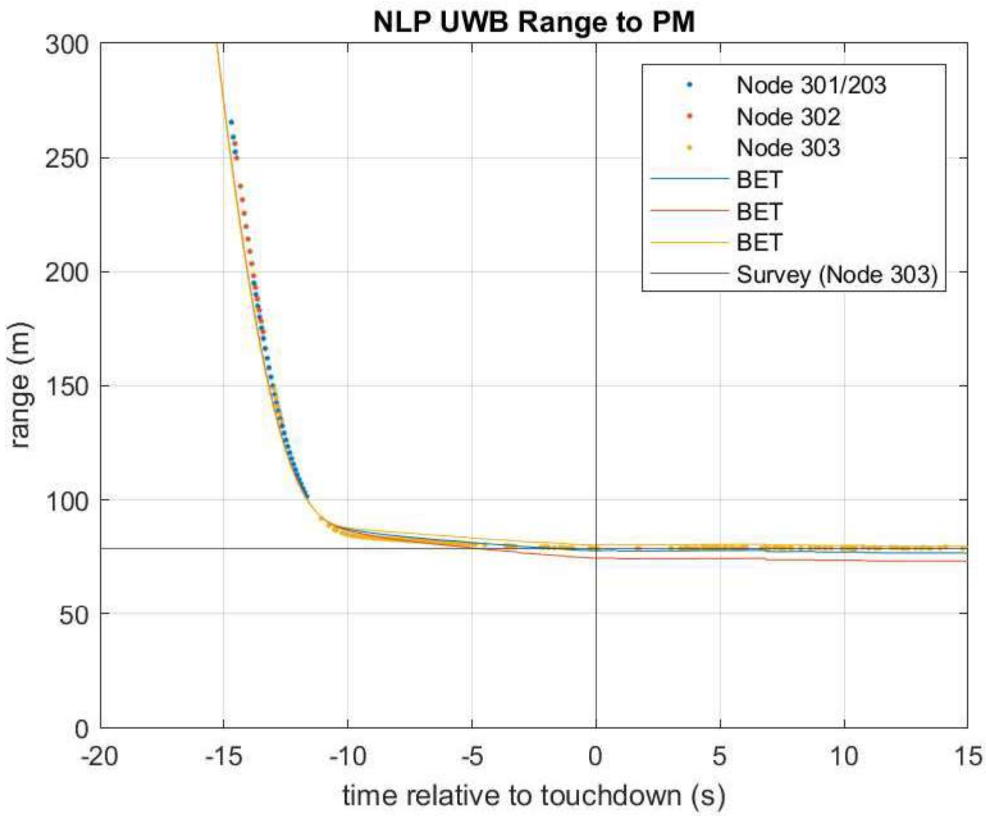

Figure 10: Range from the UWB at the landing pad to the PM ring-fin UWB a measured and as predicted from the BET.

Early in the descent, all the UWB measured longer ranges that the BET predicted, as shown in Figure 11. However, the range estimates produced by the UWB were highly consistent with each other. Given the well understood inaccuracy of GNSS-derived altitude measurements and that the UWB measurements are internally consistent, the error in Figure 11 is most likely the result of GNSS measurement error in the BET.

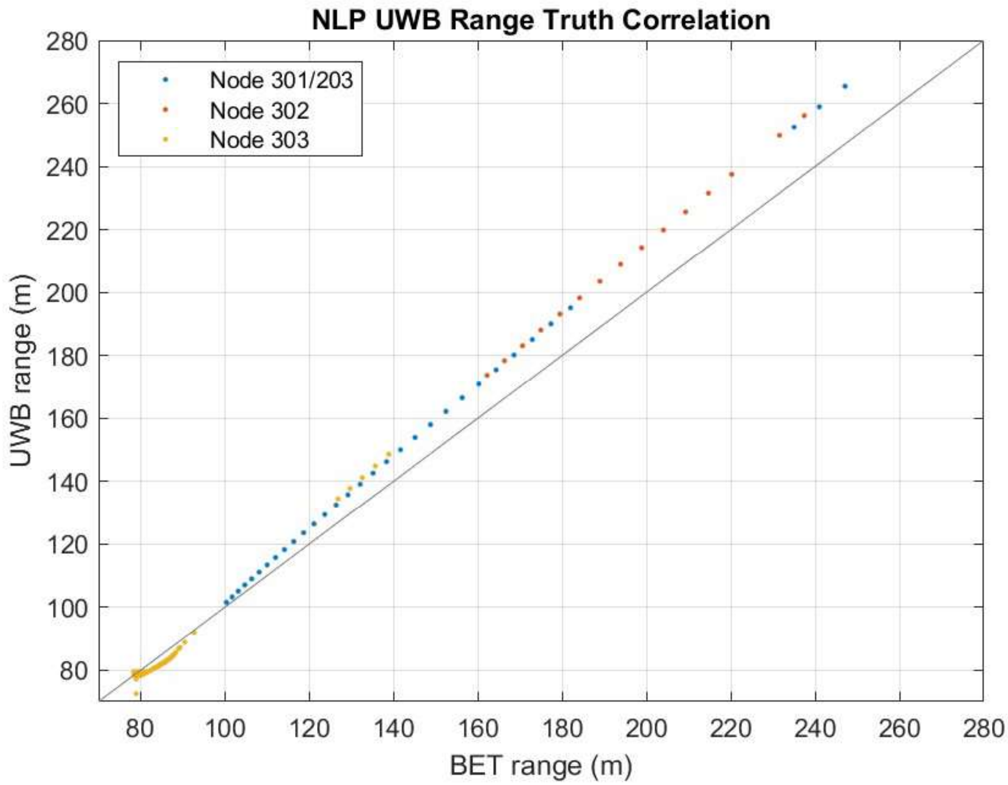

Figure 11: Range from the UWB at the landing pad to the PM ring-fin UWB against BET-derived estimates of the same range.

There is no evidence that the PM engine plume or the dust/debris kicked up by landing had any impact on the UWB performance. No UWB was intermittent during touchdown, and cutoff appears to be correlated with increasing azimuth (though there did not appear to be an obvious cutoff angle, per Figure 12). It is not clear why UWB 303 was able to remain connected to the PM ring-fin UWB to a much higher azimuth angle than the other two UWBs at the landing pad.

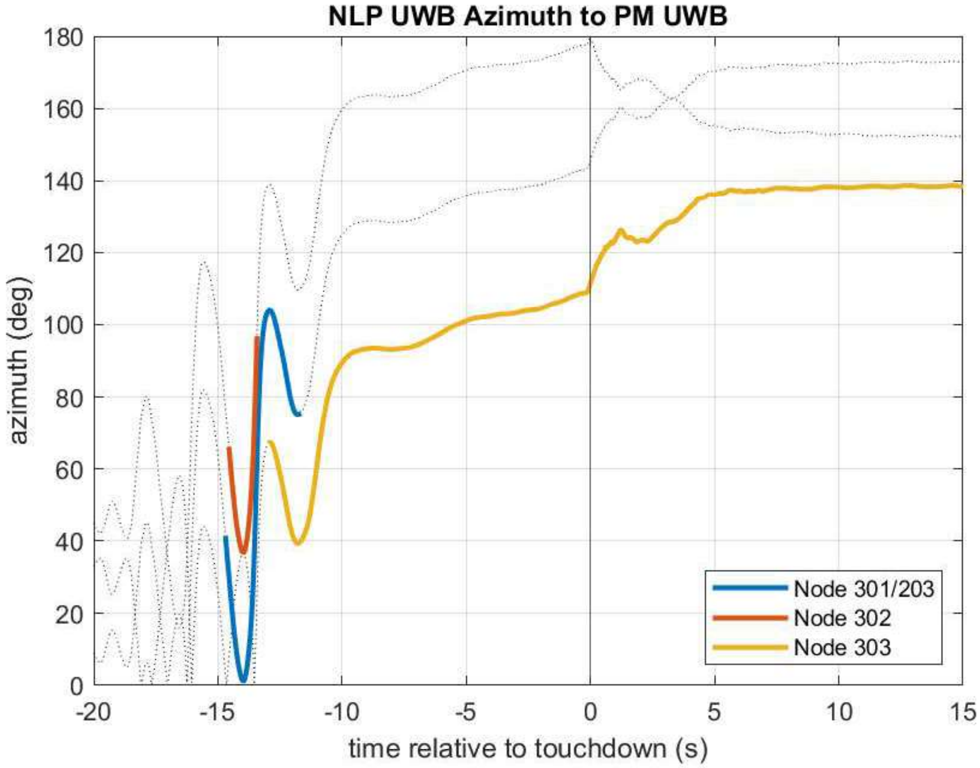

Figure 12: Azimuth angle from the PM ring-fin UWB to the landing pad UWBs, with the sections where measurements were available highlighted.

Range measurements from the landing pad UWB generally tracked the BET predicted range well, with low noise. After landing, the PM ring-fin UWB was left on for several minutes. Figure 13 shows the range measured by the UWB 303, the range predicted by the BET (which is derived primarily from GPS), and the range predicted by a post-recovery survey of the PM touchdown position. The UWB provided more accurate range and more stable range measurements than the BET. Interestingly, the range measurements for the UWB were multi-modal, with clear bands of measurement at increments of 27 cm.

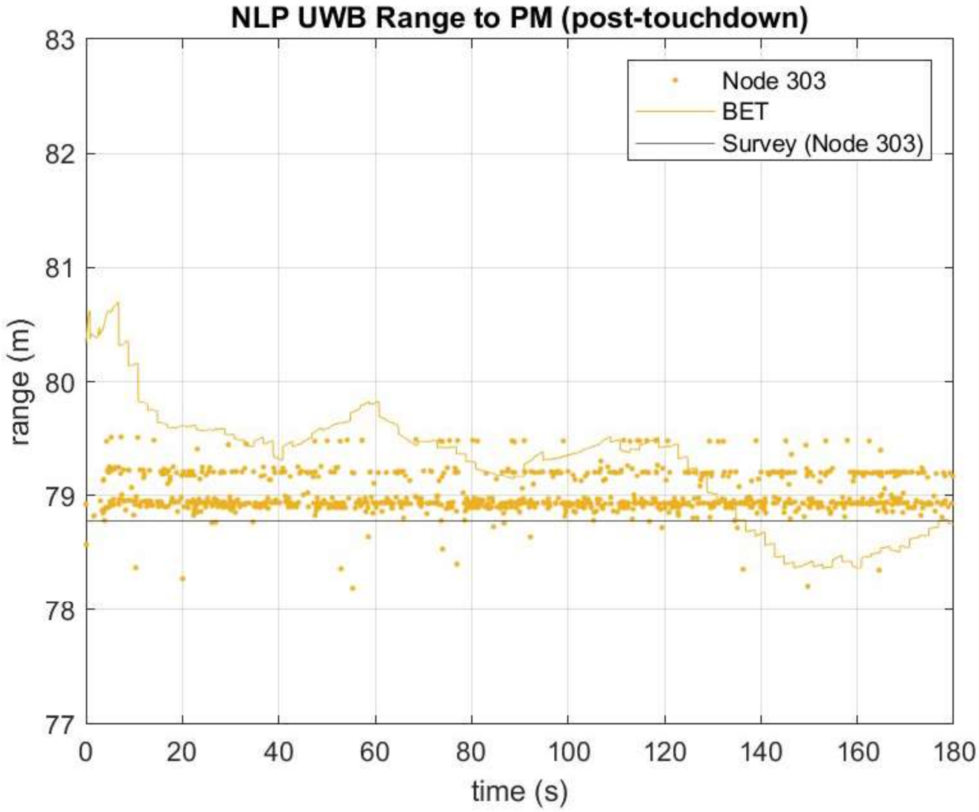

Figure 13: Range from Node 303 at the landing pad to the PM ring-fin UWB after touchdown as measured, as predicted by the BET, and as predicted from a post-landing survey.

3.3. **Conclusions and Recommendations**

While the configuration of UWB employed in this experiment imposed limitations on the observability of the PM UWB during landing, we were able to demonstrate the potential of UWB as a valuable landing sensor. The UWB sensors operated at over 250 m range and provided significantly better range estimation than the GNSS-derived BET.

Based on these results, a second UWB placed on the opposite side of the PM and an additional UWB located at the landing pad would have allowed at least three UWB pairs to perform ranging regardless of the PM orientation during descent. The PM UWB was observable consistently at azimuth angles of at least 90°, demonstrating that a relatively small number of low-cost sensors could provide full landing pad coverage.

The configuration of the UWB installations in this experiment was primarily driven by expediency. Placing the landing pad UWB closer to the edge of the landing pad and placing the PM UWB lower on the vehicle would increase the effective range of the sensors and increased their efficacy as landing sensors. Careful design of the antenna and addition of a ground plane for the ground UWB should be considered to potentially eliminate multipath from the landing pad.

4. VISION-BASED RPO SENSING OBJECTIVE

4.1. Overview

The vision-based proximity sensing experiment was designed to test low-cost fiducial markers with a low-cost machine vision camera as a proximity sensor during separation of the New Shepard Propulsion Module and Crew Capsule in space relevant environments and illumination.

Four unique AprilTags [2] fiducial markers were made of rubber. The fiducials were numbered 0, 2, 3, and 5, corresponding to the numbers encoded in the patterns from the 16h5 AprilTag family. These were then adhered to the PM tabletop at the access panel outer corners to distribute them over as large a bearing baseline as possible. A machine vision camera installed in the aft compartment of the Crew Capsule behind an aft-facing window in the base heat shield provided imagery of the fiducial markers during separation.

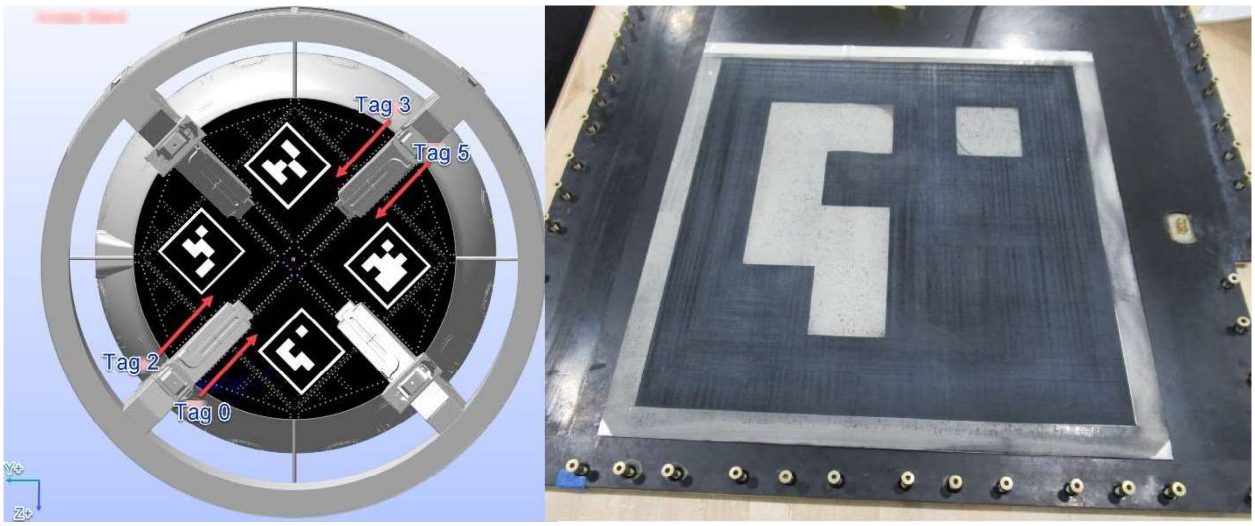

Figure 14: Four AprilTags fiducials made of automotive-grade rubber were installed on the PM tabletop.

The crew capsule camera intrinsics and extrinsics were calibrated prior to the mission using a ChArUco board equipped with metrology targets. Residual distortion averaged approximately 0.5 px and was largely uncorrelated.

During the mission, the machine vision camera recorded continuously, with videos stored in 15 min segments. The video segment containing the PM and CC separation was post-processed to detect the AprilTags and determine the relative bearings from the CC camera to the fiducials. Note that, while the vehicle mission profiles were essentially the same, the VBN RPO sensing experiment flew on a different mission (NS-24, 2023-12-19) and different PM and CC than the UWB experiments.

4.2. Key Results and Findings

Two video files contained the portion of the CC video in which the fiducials were visible. The video files were stitched together, distortion corrected, and processed through an AprilTags detector. Due to the low sun-angle and the pitch rate of the PM at separation, a deep shadow obscured all but Tag 0 after only a few seconds. To increase the window of detectability for the AprilTags, a contrast-limited adaptive histogram equalization (CLAHE) algorithm (before and after displayed in Figure 15) was applied to video frames before AprilTags detection, which increased the detection window of the fiducials by several seconds. One frame of the original, distortion corrected, video with detected AprilTags is shown in Figure 16.

Figure 15: Original and contrast-enhanced grayscale image from the CC camera.

Figure 16: AprilTags detected in one frame of the CC aft camera.

All four fiducials were detected at least once after separation, but three of the fiducials were shadowed or obscured after only a few seconds. Figure 17 shows the timespan each fiducial was detected over the course of the video. Tag 0 was not initially detectable, but once detected, remained detectable to almost 40 m, significantly beyond the 25 m range we had anticipated. Maximum predicted detection range was based on a previously derived, conservative limit of 9 camera pixels per fiducial "pixel". In practice AprilTags can be detected down to 6 camera pixels per fiducial "pixel" in optimal conditions.

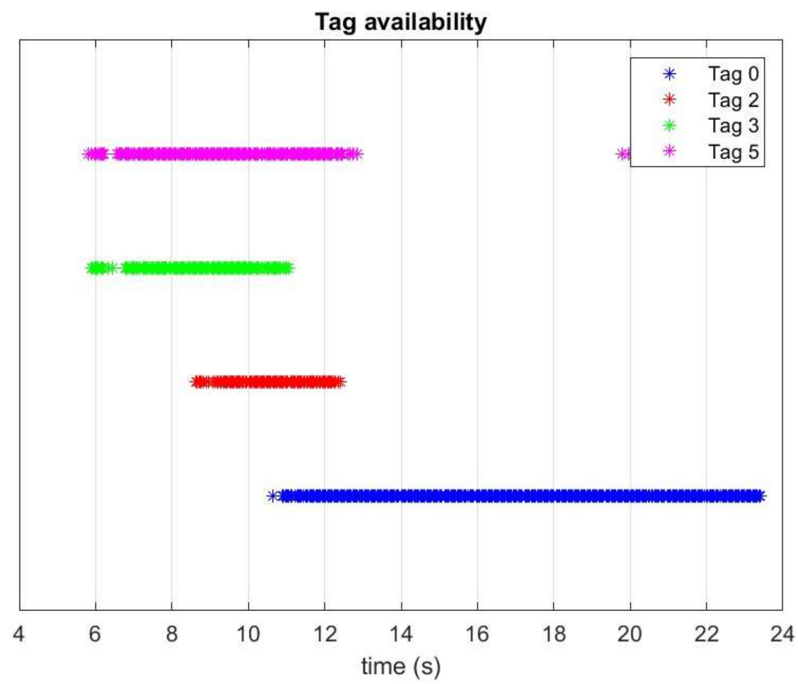

Figure 17: AprilTag detectability windows.

Figure 18 shows the position of the fiducial centers, after outliers are removed. Outliers were rejected based on:

- the AprilTags detector quality metric;
- tag area changing too abruptly; or
- tags not being detected in at least three consecutive frames.

Outlier tags tended to flicker and change size at random in the camera field-of-view. The trace of the fiducial centers trends towards a center point as the CC pulls away from the PM. Even after removing most outliers, several significant outliers do remain.

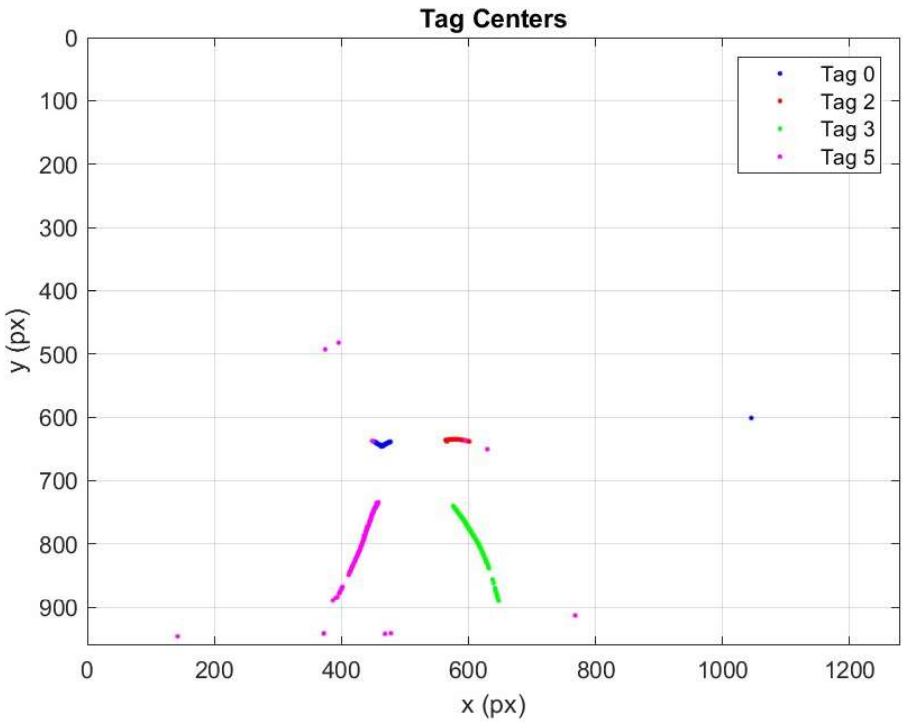

Figure 18: Detected AprilTag positions in the camera field-of-view.

We used a simple nonlinear least squares approach to triangulate the relative position of the CC and PM. The fit variables were the relative position of the camera to the propulsion module and the quaternion of the relative orientation of the camera to the propulsion module. An additional pseudo-measurement was used to constrain the quaternion to unit magnitude, removing the extraneous degree of freedom from the quaternion parameterization. Camera extrinsic calibration permitted the relative pose of the Crew Capsule to the Propulsion Module to be derived from the camera pose estimate.

The triangulated pose produced generally accurate range estimates, but horizontal offsets (which are less observable) were sensitive to variation in the relative orientation estimate. Figure 19 shows the estimated pose using the centers of each tag in each frame where at least three fiducials were visible. Fiducial centers were preferred in this scenario because they average out noise in the detection of the tag corners. The relative orientation estimate was most accurate about the vehicle roll axis (denoted 'x' in Figure 2Figure 19) which is the most observable orientation component with this fiducial configuration. Estimation of vehicle relative tilt is coupled with the horizontal position offset, making those states more difficult to determine accurately. Range was estimated to be within 0.5 m (around 1.5%) of the BET estimate. Outliers in the pose estimate in Figure 19 occurred when outlier tag detections were included in the triangulation.

Figure 20 shows how the relative x-position estimate (which is also the range, up to a small error for the horizontal offset) from the VBN algorithm compares to the BET x-position offset. The error between the two consists primarily of a fixed bias with little to no scale error apparent.

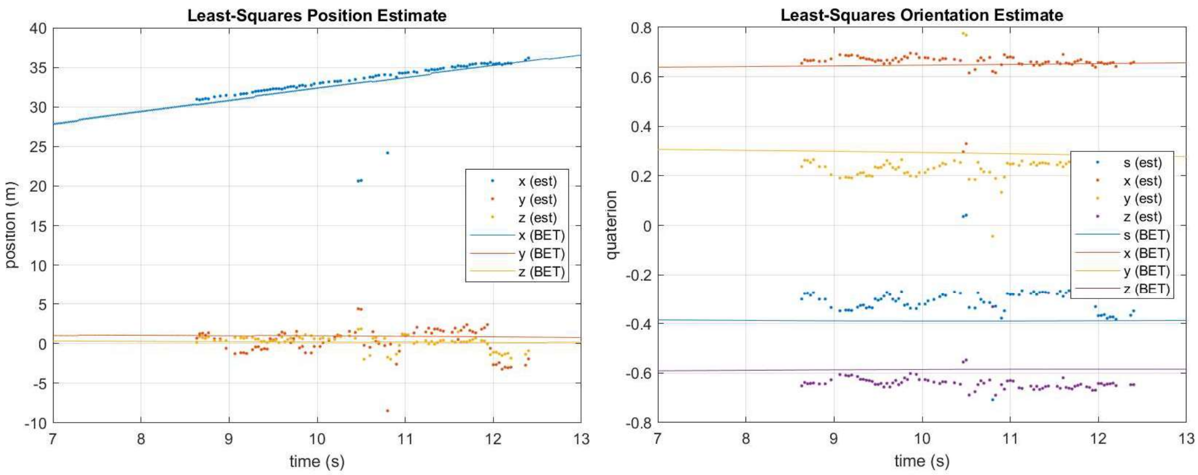

Figure 19: Position and orientation (as a quaternion) of the CC camera triangulated from at least 3 fiducial detections.

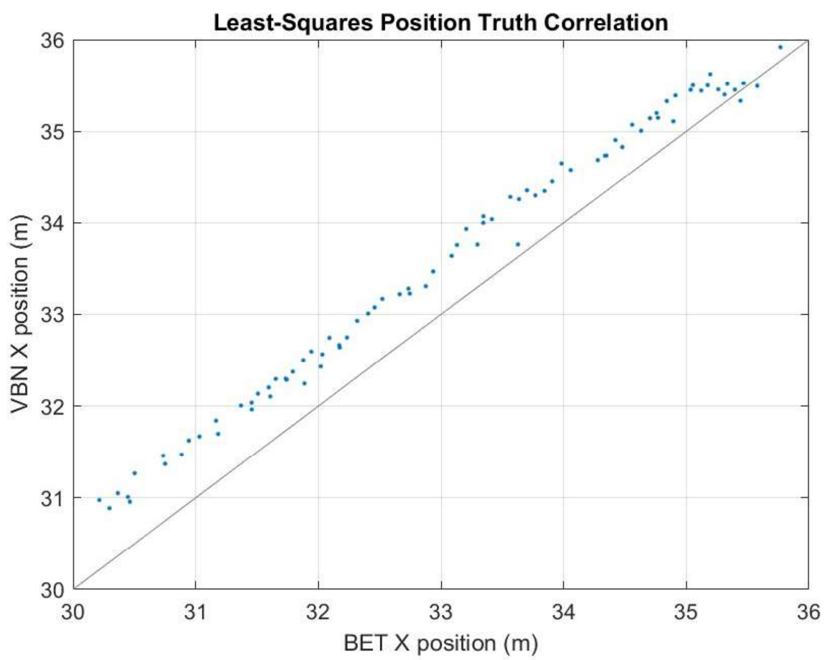

Figure 20: VBN x-position (a strong proxy for range) plotted against the BET estimated x-position of the VBN camera relative to the PM.

4.3. **Conclusions and Recommendations**

Despite the short duration that most of the fiducials were unshaded, we demonstrated that vision-based navigation can be used to produce accurate relative pose estimates in proximity operations. Shadowing aside, at least one AprilTag fiducial remained detectable to well beyond the range at which the installation would have provided a useful pose estimation baseline.

The raw outputs of the AprilTags algorithm produced many outliers. Applying a small number of relatively simply heuristic filters, however, reduced the outliers to manageable levels. Further filtering, including chi-square rejection would likely produce highly reliable measurements. Use of a denser tag family (we used a 4x4 pixel AprilTag design to maximize detection range) would potentially reduce the number of false detections as well, at the expense of detection range for a fixed fiducial size.

Estimation of vehicle pose was ill-conditioned with respect to vehicle tilt in this scenario because all the fiducials were located on a single plane perpendicular to the camera. If range estimation is not the primary consideration, a dedicated VBN integration placing some tags on a separate plane would improve observability of tilt, and of position offsets in the camera plane, which are highly coupled to the tilt estimate. In addition to estimating pose from the tag centers, we also performed pose estimation from the fiducial corners. While this approach did not produce meaningful benefits in this application (i.e., where the fiducials were all perpendicular to the camera), had any of the fiducials been significantly inclined relative to the camera, the fiducial corners would have increased pose estimation quality.

Adequate illumination proved a key constraint on the use of passive fiducials during this demonstration. Although contrast-enhancement algorithms increased the effective detection range, several fiducials ceased to be detected after being shadowed by the PM ring-fin and its supports, well before they could be lost to resolution constraints. The PM tabletop provides a particularly challenging environment for lighting, however. In a production application, care should be taken to avoid placing fiducials away from equipment that could cast large shadows, or to provide active illumination.

5. PROGRAM LEVEL CONCLUSIONS AND RECOMMENDATIONS

5.1. Conclusions

Referring to Section 1.11.2, the primary program objectives were:

- Sensors to operate on the vehicle and in space relevant environments.
- Sensors to record data throughout vehicle separation, and, for the UWB sensors only, throughout landing.
- Collect flight data that can be used to estimate the relative position of the PM and CC.
- Operational range and accuracy of each sensor type to be determined.

The task summaries in Sections 2, 3, and 4, described in detail how those objectives were met. Range and accuracy of both the UWB and VBN proved to be highly sensitive to how they are integrated into the vehicle platform. Limitations on where payloads could be placed on New Shepard compromised the performance of both sensors relative to a dedicated sensor integration design; these results should be considered conservative bounds on the performance of UWB and VBN as relative sensors for proximity or landing.

Care should be taken in integration of UWB sensors for RPO applications to avoid multipath interference between sensors and provide direct antenna-to-antenna line-of-sight without intervening structure. While the UWB sensors provided accurate range information during separation, noise was a concern, and the maximum range of the integration was significantly less than expected. The landing UWB experiment demonstrated that UWB are capable of sensing at much longer range when less vehicle structure is in the way.

Similarly, integration was the primary limiting factor in the performance of the VBN RPO experiment. VBN fiducials should be integrated to minimize the risk of shadowing, and artificial illumination should be provided if operations in Earth's umbra are required. AprilTags provided a straight-forward fiducial design and detection algorithm that worked reliably to longer than the predicted range.

5.2. Recommendations

The flight tests in this effort demonstrated that the technologies under investigation operate successfully in space proximity and landing environments. However, further investigation into measures that could improve reliability and outlier/noise rejection is warranted.

We recommend performance tests of the UWB sensors with directional antenna and matching ground plane to measure potential range improvements in UWB sensing. Experiments at the New Shepard landing pad using a personnel lift would also allow us to test design improvements to reduce multipath interference in landing sensor applications.

We also recommend performing a comparative study of the relative abundance of false detections of AprilTags in dense visual scenes between different AprilTags families (4x4, 5x5, and 6x6 pixel) to allow informed trades on detection range (which will decrease for a fixed fiducial size as fiducial density increases) against robustness to false detections.

A. PHOTOS

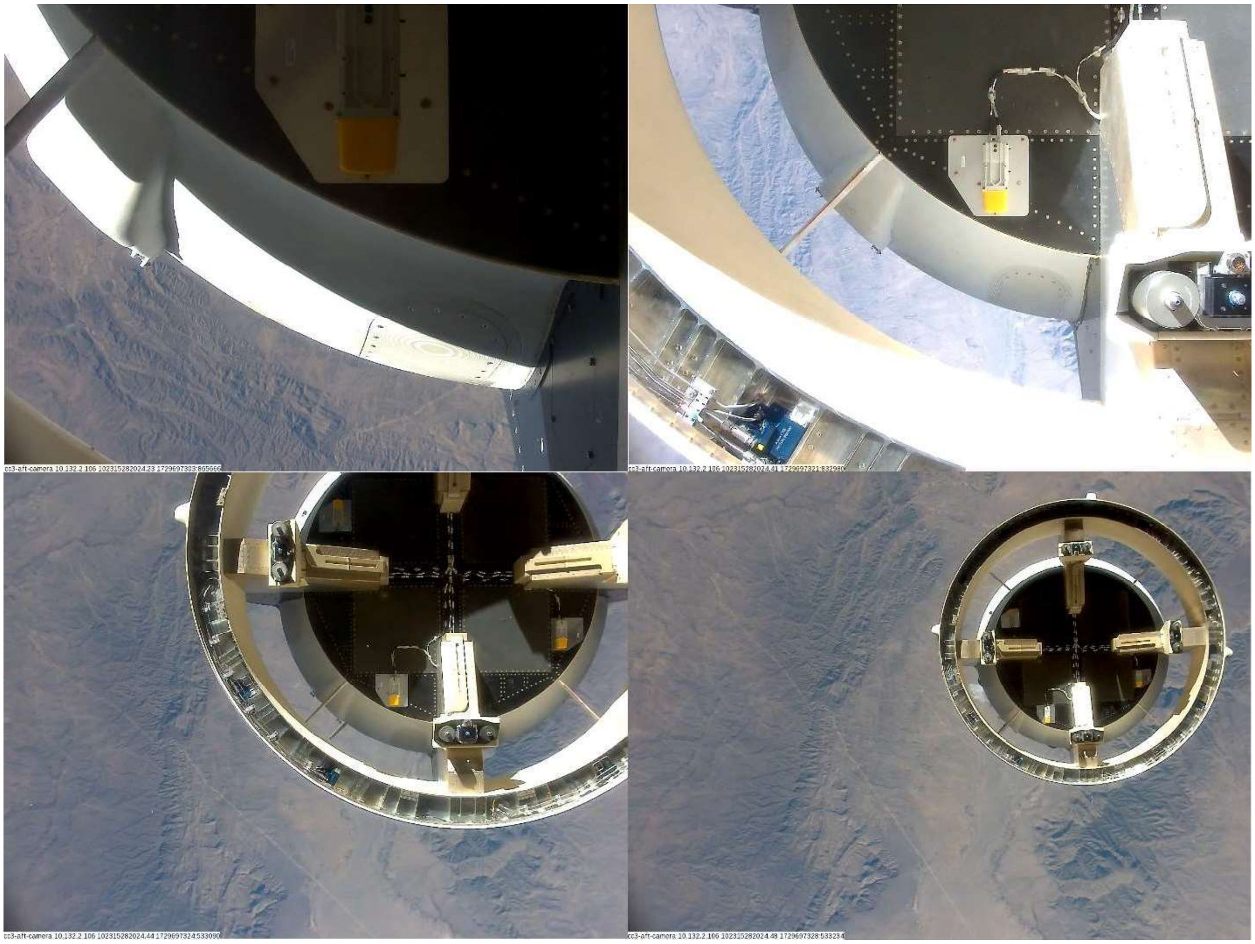

Figure 21: PM Tabletop UWB installation viewed from the CC during separation.

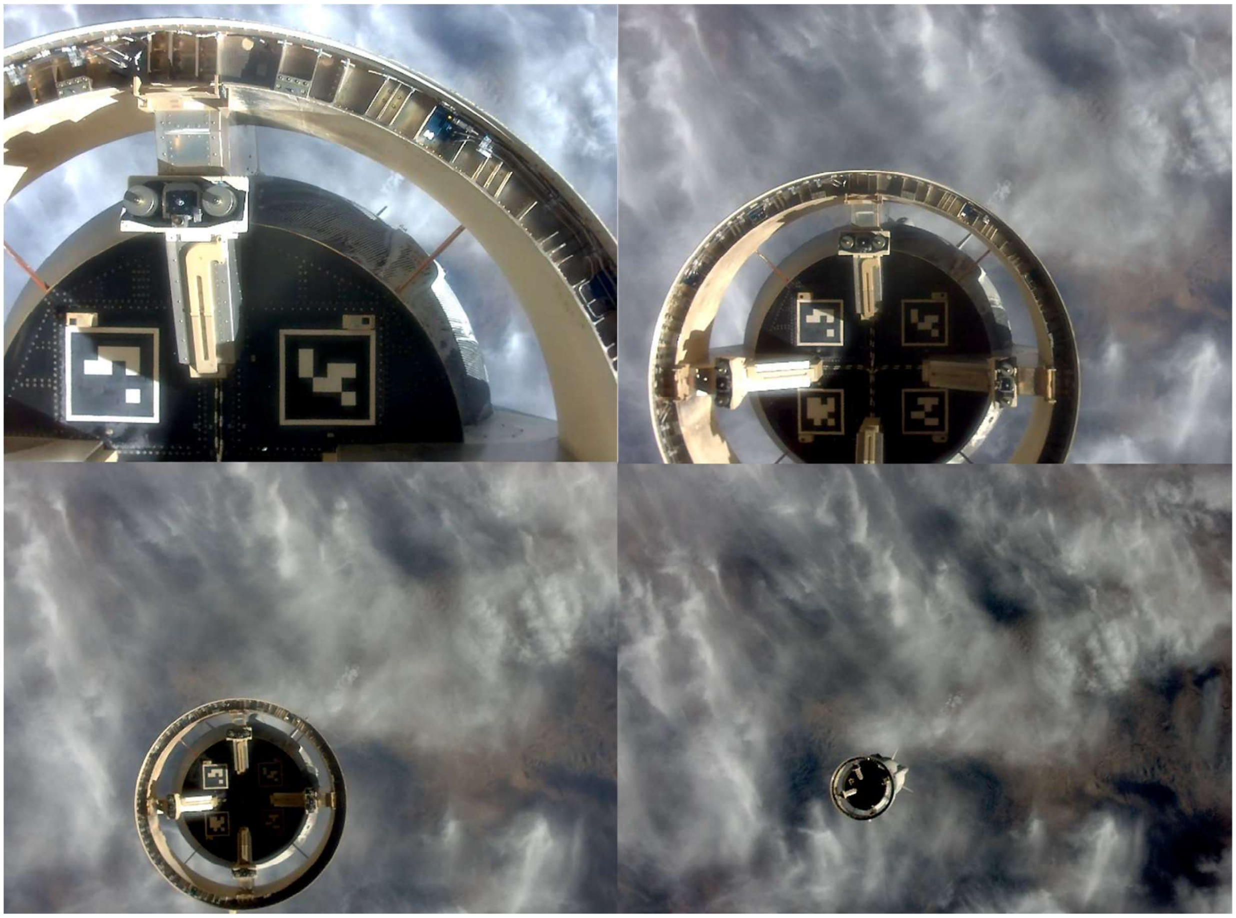

Figure 22: PM AprilTag fiducials viewed from the CC during separation.